Enhancement of thermoelectric properties by lattice softening and energy band gap control in Te-deficient InTe$_{1-\#}$

Song Yi Back, Hyunyong Cho, Young-Kwang Kim, Seokyeong Byeon, Hyungyu Jin (iD), Kunihito Koumoto, and Jong-Soo Rhyee (iD)

ARTICLES YOU MAY BE INTERESTED IN

A practical field guide to thermoelectrics: Fundamentals, synthesis, and characterization
Applied Physics Reviews **5**, 021303 (2018); https://doi.org/10.1063/1.5021094

Characterization of Lorenz number with Seebeck coefficient measurement
APL Materials **3**, 041506 (2015); https://doi.org/10.1063/1.4908244

Unique nanostructures and enhanced thermoelectric performance of melt-spun BiSbTe alloys
Applied Physics Letters **94**, 102111 (2009); https://doi.org/10.1063/1.3097026

Enhancement of thermoelectric properties by lattice softening and energy band gap control in Te-deficient InTe$_{1-\delta}$

Song Yi Back,[1] Hyunyong Cho,[1] Young-Kwang Kim,[2] Seokyeong Byeon,[3] Hyungyu Jin,[3] Kunihito Koumoto,[1,4] and Jong-Soo Rhyee[1,a]

[1]*Department of Applied Physics and Institute of Basic Sciences, Kyung Hee University, Yongin 17104, Korea*
[2]*Department of Materials Science and Engineering, Pohang University of Science and Technology, Pohang 37673, South Korea*
[3]*Department of Mechanical Engineering, Pohang University of Science and Technology, Pohang 37673, South Korea*
[4]*Toyota Physical and Chemical Research Institute, Nagakute 480-1192, Japan*

The InTe has intrinsically low lattice thermal conductivity κ_L originating from the anharmonic bonding of In^{1+} ion in the lattice, which scatters the phonons. Here we report the enhancement of thermoelectric properties in Te-deficient InTe$_{1-\delta}$ ($\delta = 0$, 0.01, 0.1, and 0.2) polycrystalline compounds by lattice softening and energy band gap opening. Te-deficiency gives rise to more weak chemical bonding between In^{1+} atoms and In^{3+}Te^{2-} clusters than those of pristine InTe, resulting in the reduction of κ_L near the room temperature. The weak ionic bonding is confirmed by the increase of lattice volume from the X-ray diffraction and lattice softening by the decrease of Debye temperature with increasing Te-deficiency. We observed the low lattice thermal conductivity κ_L of 0.53 W m^{-1} K^{-1} at 300 K for InTe$_{0.99}$, which is about 25 % decreased value than those of InTe. The Te-deficiency also induces energy band gap so that the electrical resistivity and Seebeck coefficient are increased due to the decrease of carrier concentration. Temperature-dependent thermoelectric properties shows the high Seebeck coefficient at high temperature and high electrical conductivity near room temperature, resulting in the temperature-insensitive high power factor $S^2\sigma$ over a wide temperature range. Owing to the temperature-insensitive high power factor and intrinsic low lattice thermal conductivity by Te-deficiency, the thermoelectric performances of figure-of-merit ZT and engineering ZT_{eng} are enhanced at mild temperature range ($\leq$550 K). *© 2018 Author(s). All article content, except where otherwise noted, is licensed under a Creative Commons Attribution (CC BY) license (http://creativecommons.org/licenses/by/4.0/).* https://doi.org/10.1063/1.5063274

I. INTRODUCTION

Thermoelectricity is very promising technology for an energy harvesting and environmentally friendly cooling technology because thermoelectric materials can directly convert waste heat into electricity and drive temperature difference at two ends of thermoelectric materials that is applied to the solid state cooling. The performance of thermoelectric (TE) materials is defined by the dimensionless figure-of-merit $ZT = S^2\sigma T/(\kappa_{el} + \kappa_L)$, where S, T, σ, κ_{el}, and κ_L are the Seebeck coefficient, absolute temperature, electrical conductivity, electronic thermal conductivity, and lattice thermal conductivity, respectively. In order to achieve the high performance, it needs to be increased the power factor $PF = S^2\sigma$ as well as to be decreased the lattice thermal conductivity κ_L.

---

[a]E-mail address: jsrhyee@khu.ac.kr (JSR).

8, 115227-1

The enhancement in PF has been reported through the formation of resonant level,[1] the band convergence,[2] and the carrier filtering effect.[3] The effective way to reduce κ_L is to induce phonon scattering by nano-structuring,[4] anharmonicity of phonons,[5] and nano-scale grain boundary,[6] nano-precipitation,[7] and point defects.[8] The optimization of carrier concentration for materials with intrinsically low κ_L are good approach for high efficiency of TE materials. Recent investigation shows that the phonon interaction with lone pair electrons results in low lattice thermal conductivity due to lattice anharmonicity. For example, the cubic I-V-VI$_2$ (where I = Cu, Ag, Au or alkali metal; V = As, Sb, Bi; and VI = Se, Te) compounds have intrinsically low κ_L due to strong anharmonicity originating from the lone-pair electrons of the group V atoms.[9,10] The s^2 electrons on the group V atoms do not form sp^3 hybridized bonds and are isolated, which can be easily distorted by lattice vibrations leading to the lattice anharmonicity.[10] The enhancement in TE properties of AgSbSe$_2$-based compounds have been mainly focused on the carrier concentration optimization by various dopants such as Ge,[11] Zn,[12] Sb-deficient[13] and other doping materials.[14,15]

InTe exhibits the ultra low κ_L due to rattling vibrations of In^{1+} atoms with the $5s^2$ lone pair electrons.[16] The structure of InTe is the tetragonal with the space group $I4/mcm$ composed of In$^+$-In^{3+}-Te^{2-}.[17] The In^{3+} and Te^{2-} ions form sp^3 hybridized bonding but the In^{1+} ions are loosely bonded ionically to the In^{3+}-Te^{2-} chains. Here, we investigated the thermoelectric properties on the Te-deficiency effect in p-type InTe$_{1-\delta}$ (δ = 0.0, 0.01, 0.1, and 0.2) compounds. We observed the enhancement of power factor over a wide temperature range due to the increase in Hall mobility, while the compounds maintain intrinsically low κ_L of 0.53 W m^{-1} K^{-1} at 300 K for InTe$_{0.99}$ which is about 25 % lower value than those of pristine InTe. The low κ_L in Te-deficient compounds may come from the weak bonding strength, confirmed by the Debye temperature and lattice parameters. Owing to the improved power factor and decreased lattice thermal conductivity, the Te-deficient compounds of InTe$_{1-\delta}$ enhances ZT and engineering ZT_{eng} values over a wide temperature range.

II. EXPERIMENTAL AND THEORETICAL DETAILS

A. Synthesis

The Te-deficient InTe$_{1-\delta}$ compounds were prepared by direct melting and hot press sintering. Stoichiometric elements of In (99.999 %) and Te (99.999 %) shots of InTe$_{1-\delta}$ (δ = 0.0, 0.01, 0.1, and 0.2) were loaded in quartz ampoules and sealed under a high vacuum 10^{-5} torr environment. The quartz ampoules were heat treated in a rocking furnace at 850°C over 24 hours and slowly cooled to room temperature for 30 hours. The ingots were pulverized into fine powders in an agate mortar and the powders were sintered by a vacuum hot-press sintering machine in a graphite mold at 510 °C for 1 h under a uniaxial pressure of 50 MPa. The sample densities of the sintered compounds have a range from 6.19 g/cm^3 to 6.23 g/cm,^{3} which is close to the theoretical density (6.29 g/cm^3) with high relative densities (98 ~99 %). The sintered samples were cut and polished for thermoelectric properties measurement. We measured the samples along the parallel direction to the uniaxial direction of the hot-press.

B. Measurements

The structural properties were identified by the powder X-ray diffraction (XRD) using a Cu Kα radiation (D8 Advance, Bruker, Germany). The heat capacity C_p measurements for the estimation of Debye temperature Θ_D were conducted by a physical property measurement system (PPMS, Dynacool-14T, Quantum Design, U.S.A.). The electrical resistivity ρ and Seebeck coefficient S measurement were carried out by a ZEM-3 (ULVAC, Japan) under 5N helium environment. The thermal diffusivity λ was measured by a laser flash method (LFA-456, Netzsch, Germany) and thermal conductivity κ was obtained by the relation $\kappa = d_s \lambda C_p$, where d_s, λ, and C_p are the sample density, thermal diffusivity, and specific heat, respectively. The Hall coefficient R_H for carrier concentration and Hall mobility μ_H were measured by a PPMS using a four-probe contact method with the magnetic field sweeping from −5 to 5 T.

C. Theoretical details

In order to investigate the electronic band structure, we used the VASP code[18–20] and the projector-augmented plane wave (PAW) method[21] within the Perdew-Burke-Ernzerhof generalized gradient approximation (GGA)[22] for the exchange-correlation functional. For structural relaxations, the reciprocal-space energy integration was performed by the Methfessel-Paxton technique.[23] We used a 9×9×9 k-points mesh and a 520 eV energy cutoff of the wave function. The convergence criterions of the electronic self-consistency for energy and forces set were chosen as 10^{-6} eV and 10^{-2} eV/Å, respectively. Magnetism was included by considering spin-polarized calculations. The calculations of the total energies with structure relaxations were performed by the tetrahedron method incorporating a Blöchl correction.[24] The electronic band structure was obtained from Kohn-Sham eigenvalues estimated by a static selfconsistent calculation along high symmetry lines in the Brillouin zone.[25]

III. RESULTS AND DISCUSSION

The X-ray diffraction (XRD) patterns and lattice volumes of Te-deficient $InTe_{1-\delta}$ ($\delta = 0.0, 0.01$, 0.1, and 0.2) compounds are presented in Fig. 1(a) and (b), respectively. The diffraction peaks of all the compounds represent single phase with the tetragonal structure (space group I4/mcm) with
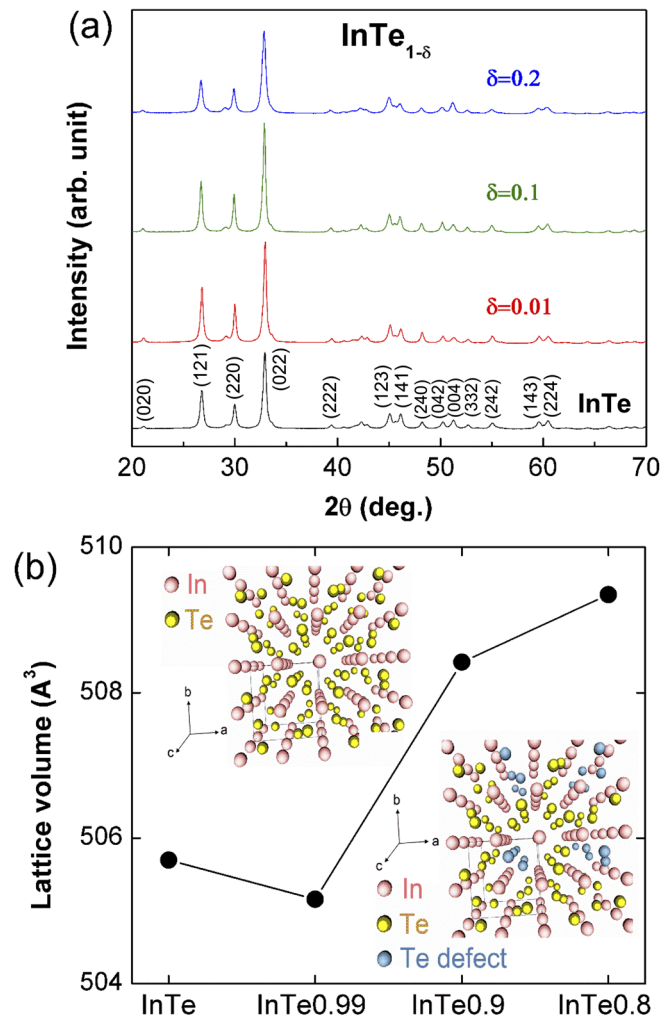

FIG. 1. X-ray diffraction patterns (a) and lattice volume (b) for $InTe_{1-\delta}$ ($\delta = 0.0, 0.01, 0.1,$ and 0.2) compounds.

TABLE I. Lattice parameters and lattice volume of the InTe$_{1-\delta}$ (δ = 0.0, 0.01, 0.1, and 0.2) compounds.

δ	a (Å)	c (Å)	V (Å)
0.00	8.425 (8)	7.123 (1)	505.70
0.01	8.425 (9)	7.115 (3)	505.16
0.10	8.443 (7)	7.131 (1)	508.42
0.20	8.445 (6)	7.141 (0)	509.35

no other impurity peaks. The lattice parameters are listed in Table I. The a-axis lattice parameters are monotonically increased with increasing Te-deficiency. The c-axis lattice parameters are also increased except the case of δ = 0.01 compound. Inset of Fig. 1(b) presents the crystal structure of stoichiometric InTe (upper left) and InTe$_{1-\delta}$ (lower right) compounds, where the Te-defect is indicated as sky blue ball. In many cases, self-defect structure shrinks crystal lattice resulting in the decrease of lattice parameters. On the other hand, the increasing of lattice parameters and lattice volume indicates that the Te-deficiency itself decreases c-axis lattice parameter in δ = 0.01 but the bond strength becomes weak with increasing Te-deficiency.

The weak bond strength or lattice softening decreases Debye temperature Θ_D. The temperature-dependent specific heat C_p is presented in Fig. 2. It rapidly saturates at high temperature region which follows Dulong-Petit law. The Debye temperatures are estimated from the Debye T^3 law. The C_p is represented by $C_p = \gamma T + \beta T^3$ where $\beta = (12\pi^4 N_A k_B)/(5\Theta_D^3)$.[26] The Debye temperature Θ_D of the compounds are listed in Table II. The Θ_D of stoichiometric InTe is 101 K is decreased down to 92 K for δ = 0.1 and 0.2 compounds, which reveals the strengths of chemical bonding of Te-deficient compound become weaker than those of stoichiometric InTe. Both the decrease in Θ_D and the increase in lattice volume of Te-deficient compounds are originated from the weakening of bonding strength between In$^+$ atoms and In^{3+}Te^{2-} clusters.

Figure 3 presents the temperature-dependent thermoelectric properties of electrical resistivity ρ, electrical conductivity σ, Seebeck coefficient S, and power factor $PF = S^2/\rho$ of the InTe$_{1-\delta}$ (δ = 0.0, 0.01, 0.1, and 0.2) compounds. The $\rho(T)$ in Fig. 3(a) reveals the metallic behavior with temperature; decreasing with decreasing temperature. The $S(T)$ of the compounds also shows the metallic behavior with positive p-type conduction of carriers, as shown in Fig. 3(c). The $\rho(T)$ and $S(T)$ are systemically increased with increasing Te-deficiency concentrations. From the Hall resistivity measurement ρ_{xy}, we obtained the Hall carrier concentration $n_H = -1/(R_H e)$ and Hall mobility $\mu_H = R_H/\rho$, where R_H is the Hall coefficient $R_H = \rho_{xy}/H$ (H = magnetic field), as listed in Table II. For increasing Te-deficiency, the room temperature Hall carrier concentration n_H is decreased for about 5 ~6 times than those of pristine InTe. The increase of electrical resistivity and Seebeck coefficient for Te-deficient compounds is attributed from the decrease of Hall carrier concentration. Because of the decrease of
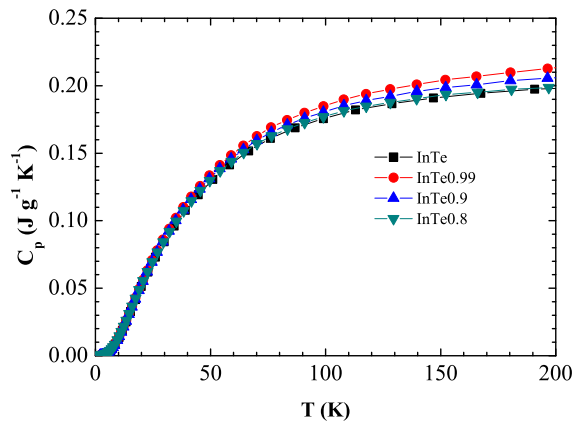

FIG. 2. Temperature-dependent specific heat C_p for InTe$_{1-\delta}$ (δ = 0.0, 0.01, 0.1, and 0.2) compounds.

TABLE II. Debye temperature Θ_D, Seebeck coefficient S, Hall carrier concentration n_H, Hall mobility μ_H, effective mass m^*, and power factor $S^2\sigma$ at room temperature of the InTe$_{1-\delta}$ (δ = 0.0, 0.01, 0.1, and 0.2) compounds.

δ	Θ_D (K)	S (μV/K)	n_H (10^{19} cm^{-3})	μ_H (cm^2 V^{-1} s^{-1})	m^* (m_e)	PF (mW m^{-1} K^{-2})
0.00	101	94.4	6.78	21	0.781	94.40
0.01	93	190.8	1.27	51	0.518	190.75
0.10	92	211.1	1.41	44	0.614	211.13
0.20	92	217.8	1.13	49	0.546	217.76

Hall carrier concentration, the Hall mobility μ_H is increased for about 2 times due to the suppression of electron-electron scattering in Te-deficient compounds.

Interestingly, the slope of the $\rho(T)$ for the Te-deficient compounds changes near 470 K in Fig. 3(a). When we examine the temperature exponent of the resistivity by $\sigma = sigma_0 + AT^n$, the temperature exponent n is abruptly changed as shown in Fig. 3(b). For pristine InTe compound, $\sigma \propto T^{-0.28}$ at $T \leq 420$ K and the exponent is decreased to $\sigma \propto T^{-1.36}$ at $T \geq 420$ K. It is known that the temperature exponent of electrical conductivity should have $n \simeq 1.5$ for ionization scattering and $n \simeq -1.5$ for acoustic phonon scattering.[27] Small critical exponent $n = -0.28$ implies the mixed scattering of ionization and acoustic phonon scattering. Abrupt increase of critical exponent $n = -1.36$ at 420 K indicates the different scattering process for enhancement of acoustic phonon scattering.

For increasing Te-deficiency concentration, the critical exponents are decreased as $n = -0.88$ ($\delta = 0.01$), $-0.91(0.1)$, and $-0.94(0.2)$, respectively, implying that the acoustic scattering is increased with increasing Te-deficiency. In addition, the crossover temperature from ionization to acoustic scattering is increased to 470 K from 420 K (InTe). Comparing to the pristine compound, the acoustic phonon scattering becomes dominant in Te-deficient compounds ($n \simeq -1.97 \sim -2.1$) at high temperature. The enhancement of acoustic scattering process can be understood by the lattice softening as

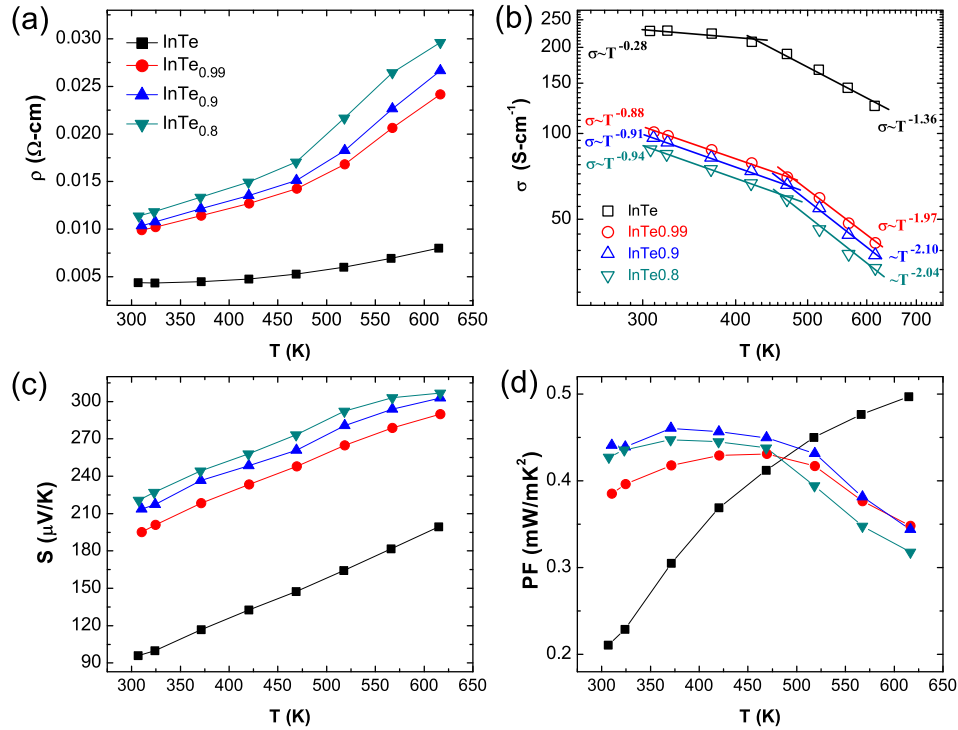

FIG. 3. Temperature-dependent thermoelectric properties for (a) electrical resistivity $\rho(T)$, (b) electrical conductivity $\sigma(T)$, (c) Seebeck coefficient $S(T)$, and (d) power factor $S^2\sigma(T)$ of InTe$_{1-\delta}$ (δ = 0.0, 0.01, 0.1, and 0.2).

we discussed in the above. The weak bond strength by Te-deficiency gives rise to increase of carrier scattering by lattice vibration.

Within the parabolic band assumption, we estimated the effective mass of carrier as following relation:[28]

$$S = \frac{8\pi^2 k_B^2}{3eh^2} m^* T \left(\frac{\pi}{3n}\right)^{2/3} \tag{1}$$

where k_B, h, e, m^*, T, and n are the Boltzmann constant, Plank constant, elementary charge, effective mass of carrier, absolute temperature, and carrier concentration, respectively. The effective masses m^* of the Te-deficient compounds are decreased ($\sim 0.55\ m_e$) comparing with the pristine compound ($0.78\ m_e$) but do not show systematic behavior with Te-deficient concentrations.

Owing to the enhancement of Seebeck coefficient at high temperature and high electrical conductivity at room temperature, the power factor showed improved value below 500 K for Te-deficient compounds, as presented in Fig. 3(d). When we compare the power factor with the Hall mobility in Table II, the enhancement in PF of Te-deficient compounds below 500 K can be attributed to the increase in the carrier mobility μ_H.

In order to understand the transport properties, we performed theoretical electronic band structures of stoichiometric InTe and InTe$_{1-\delta}$ ($\delta = 0.25$) in Fig. 4(a) and 4(b), respectively. The stoichiometric InTe exhibits band touching between conduction and valence bands at the M- and Z-points. The band touching at the points is topologically trivial because small perturbation of Te-vacancy opens energy band gap as shown in Fig. 4(b). There is a direct band gap 0.15 eV at the M-point while in-direct zero-gap is observed along the Γ-Z direction. The semimetallic zero-gap energy is consistent with the metallic behavior of $\rho(T)$. The increase of electrical resistivity and decrease Hall
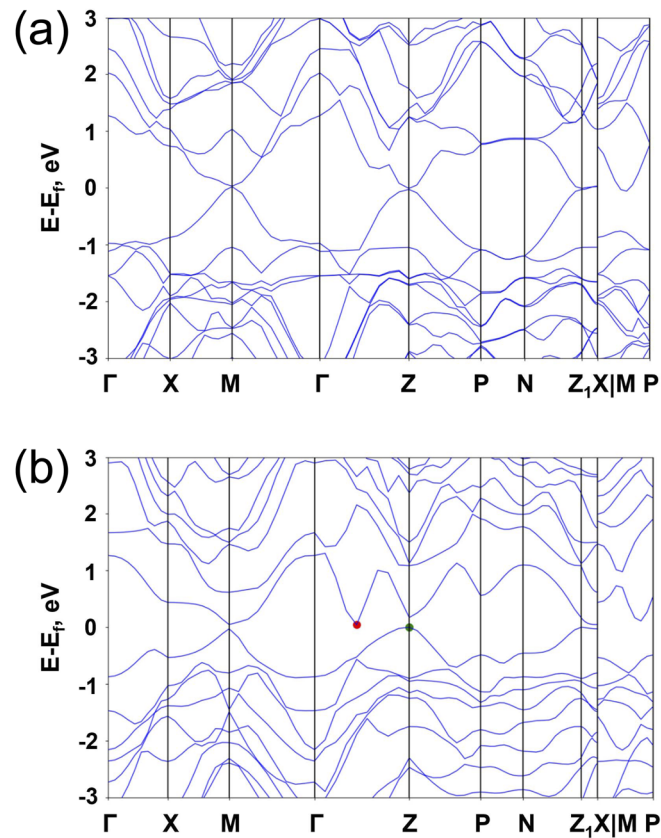

FIG. 4. Electronic band structure calculation of stoichiometric InTe (a) and Te-deficient InTe$_{1-\delta}$ ($\delta = 0.25$) (b). The symmetry k-points of BCT lattice are as follows: Γ = (0, 0, 0), M = (-1/2, 1/2, 1/2), N = (0, 1/2, 0), P = (1/4, 1/4, 1/4), X = (0, 0, 1/2), and Z = (η, η, $-\eta$), where $\eta = (1 + c^2/a^2)/4$.

carrier concentration in Te-deficient compounds than those of InTe are understood by the band gap opening at the M-point. Small Seebeck coefficient in InTe at room temperature can be ascribed by the semimetallic band character. The energy band gap opening attributes to the increase of Seebeck coefficient in Te-deficient compounds.

The Pisarenko relation of Seebeck coefficient S versus Hall carrier density n_H is depicted in Fig. 5. It relatively follows well with the single parabolic band assumption with effective mass of 0.6 m_e. The energy band dispersion at the band touching M- and Z-points can be regarded as quadratic dispersion not Dirac-like linear band dispersion. Therefore, we can apply the single parabolic band assumption for obtaining Lorenz number and lattice thermal conductivity from the Wiedemann-Franz law. In metallic or semi-metallic system, the electronic thermal conductivity follows the Wiedemann-Franz law by $\kappa_{el} = L_0 T \sigma$, where L_0 is the Lorenz number from the Drude model: $L_0 = (\pi k_B)^2/3e^2$ $= 2.45 \times 10^{-8}$ W Ω K^{-2}. Because the Te-deficient compounds have small band gap and the compounds follows single parabolic band model, we should calculate the Lorenz number within the single parabolic model with acoustic phonon scattering using following formalism:[29,30]

$$F_n(\eta) = \int_0^\infty \frac{x^n}{1 + e^{x-\eta}} dx, \tag{2}$$

where $F_n(\eta)$ is the Fermi integral and the η is the reduced electrochemical potential which is available from the temperature dependent Seebeck coefficient as given by:

$$S = \pm \frac{k_B}{e} \left(\frac{(r + 5/2)F_{r+3/2}(\eta)}{(r + 3/2)F_{r+1/2}(\eta)} - \eta \right), \tag{3}$$

The Lorenz number L in terms of temperature and η values can be calculated by fitting with Eq. (3):

$$L = \left(\frac{k_B}{e} \right)^2 \left(\frac{(r + 7/2)F_{r+5/2}(\eta)}{(r + 3/2)F_{r+1/2}(\eta)} - \left[\frac{(r + 5/2)F_{r+3/2}(\eta)}{(r + 3/2)F_{r+1/2}(\eta)} \right]^2 \right) \tag{4}$$

where the $r = -1/2$ for acoustic phonon contribution. The calculated Lorenz number $L(T)$ are depicted in Fig. 6(a). The $L(T)$ of Te-deficient compounds ($\delta = 0.01$, 0.1, and 0.2) are smaller than those of stoichiometric InTe, indicating different chemical potential energy from the InTe. Using the Lorenz number, we obtained the lattice thermal conductivity κ_L as shown in Fig. 6(b) (open symbols).

While the electronic contribution of thermal conductivity κ_{el} of stoichiometric InTe has 0.13 W m^{-1} K^{-1}, the κ_{el} of Te-deficient compounds is less than 0.05 0.13 W m^{-1} K^{-1}, indicating that the acoustic phonon contribution is significant in thermal conductivity for Te-deficient compound. When we consider the semimetallic energy band calculation in 4, the κ does not exhibit the bipolar diffusion effect at high temperature. It is caused by dominant contribution of acoustic phonon scattering in thermal conductivity.
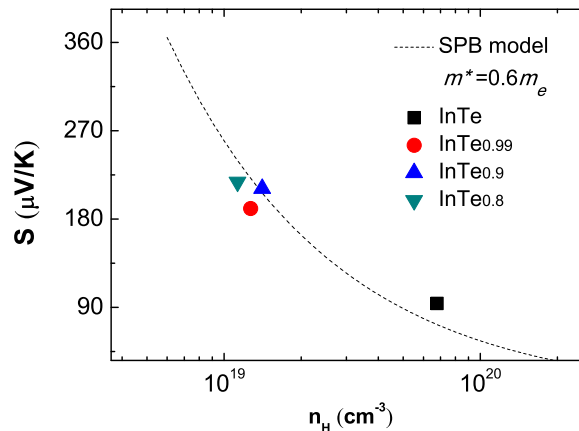

FIG. 5. Pisarenko plot for Seebeck coefficient S versus Hall carrier concentration n_H at 300 K for InTe$_{1-\delta}$ (δ = 0.0, 0.01, 0.1, and 0.2) compounds. Dashed line is the single parabolic band assumption with effective mass of 0.6 m_e (see text).
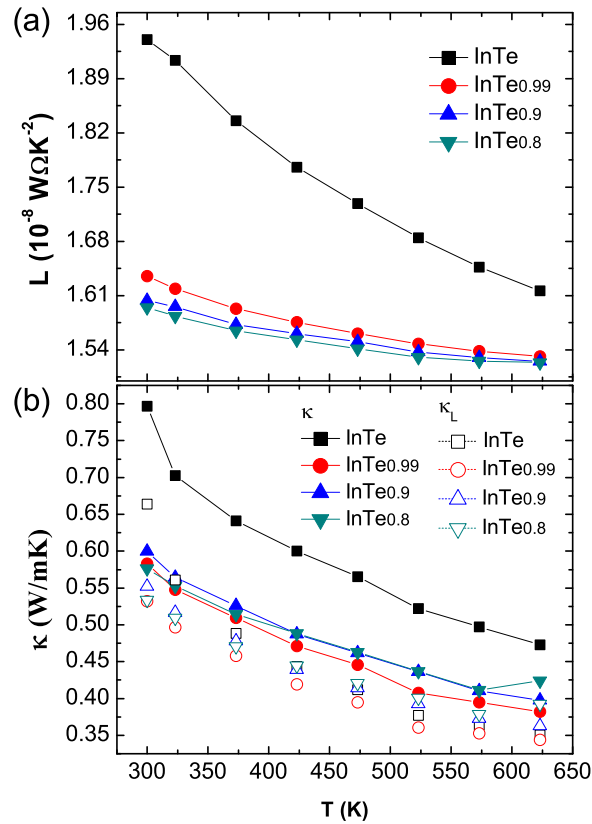
FIG. 6. (a) Temperature-dependent Lorenz number L, obtained by the single parabolic band assumption, and (b) temperature-dependent thermal conductivity κ (closed symbol) and lattice thermal conductivity κ_L (open symbol) for $InTe_{1-\delta}$ ($\delta = 0.0$, 0.01, 0.1, and 0.2) compounds.

Near room temperature, the $\kappa_L(T)$ of Te-deficient compounds is lower than the one of stoichiometric InTe. The lowest κ_L is observed 0.53 W m^{-1} K^{-1} at 300K for $\delta = 0.01$, which is about 25 % lower than those of InTe. When the heat conduction is dominated by acoustic phonon scattering, the $\kappa_L(T)$ for anharmonic Umklapp processes is represented by following relation:[31]

$$\kappa_L = A \frac{\bar{M}\Theta_D^3 \delta n^{1/3}}{\gamma^2 T} \tag{5}$$

where A is a pre-factor, $\bar{M}$ is the average mass of an atom in the crystal, δ^3 is the volume per atom, n is the number of atoms in the primitive unit cell, and γ is the high temperature limit of Grüneisen parameter.

The low κ_L values of Te-deficient $InTe_{1-\delta}$ compounds is associated with the decrease in Debye temperature, as listed in Table II because $\kappa_L \propto \Theta_D^3$. In addition, as we pointed out, the increase of lattice volume indicates lattice softening in Te-deficient compounds. The weakening of chemical bond strength owing to the Te-vacancy contributes to weak chemical bonding between In^{1+} atoms and $In^{3+}Te^{2-}$ chains, resulting in the reduction of κ_L. The acoustic phonon scattering, which is observed in the temperature exponent of $\sigma(T)$ as presented in Fig. 3(b), also related with the decrease of κ_L.

Owing to the reduction of lattice thermal conductivity κ_L and enhancement of power factor at intermediate temperature range ($T \leq 500$ K), the thermoelectric figure-of-merits ZT of the Te-deficient compounds are enhanced, as shown in Fig. 7(a). Even though high temperature ZT values of the Te-deficient compounds are lower than the pristine InTe, because of the temperature-insensitive power factor and low thermal conductivity over a wide temperature range, the engineering ZT values of the Te-deficient compounds are enhanced as shown in Fig. 7(b), where the engineering ZT_{eng} is
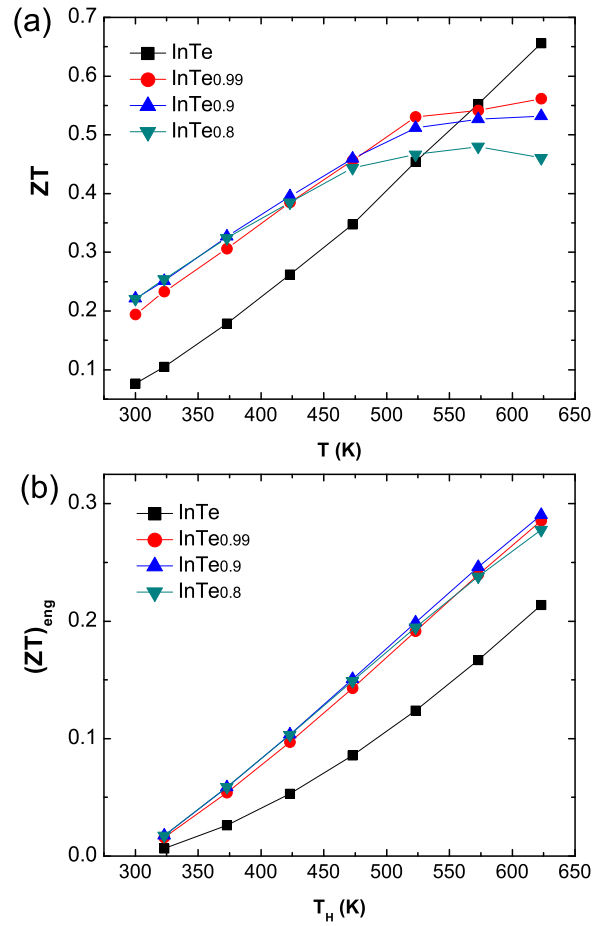
FIG. 7. (a) Temperature-dependent figure-of-merit *ZT* and (b) engineering ZT_{eng} which is defined in the text for InTe$_{1-\delta}$ (δ = 0.0, 0.01, 0.1, and 0.2) compounds.

defined by:

$$ZT_{eng} = \frac{PF_{eng}\Delta T}{\int_{T_c}^{T_h} \kappa(T)dT} \tag{6}$$

$$PF_{eng} = \frac{\left(\int_{T_c}^{T_h} S(T)dT\right)^2}{\int_{T_c}^{T_h} \rho(T)dT} \tag{7}$$

IV. CONCLUSION

In summary, we demonstrate that the Te-deficiency in InTe$_{1-\delta}$ decreases lattice thermal conductivity κ_L. The decrease of Debye temperature Θ_D and the increase of lattice volume with increasing Te-deficiency InTe$_{1-\delta}$ (δ = 0.01, 0.1, and 0.2) originate from the weakening of chemical bond strengths and lattice softening. The temperature exponent of electrical conductivity $\sigma(T)$ shows that the acoustic phonon contribution in electrical and phonon transport becomes dominant in Te-deficient compounds. For Te-deficient compounds, the energy band gap is opened while the pristine InTe has semimetallic energy band structure. Opening of small energy band gap increases Seebeck coefficient, thereby the power factor of the Te-deficient compounds are improved below 470 K. The enhancement of power factor is related with the increase of Hall mobility. Owing to the enhancement of power

factor at intermediate temperature range and reduction of lattice thermal conductivity over a wide temperature range, the *ZT* and engineering ZT_{eng} values are increased for Te-deficient compounds. This result suggests that the vacancy control and lattice softening are important criteria to enhance thermoelectric performances.

ACKNOWLEDGMENTS

[1] J. P. Heremans, V. Jovovic, E. S. Toberer, A. Saramat, K. Kurosaki, A. Charoenphakdee, S. Yamanaka, and G. J. Snyder, "Enhancement of thermoelectric efficiency in PbTe by distortion of the electronic density of states," Science **321**, 554 (2008).

[2] Y. Pei, X. Shi, A. LaLonde, H. Wang, L. Chen, and G. J. Snyder, "Convergence of electronic bands for high performance bulk thermoelectrics," Nature **473**, 66 (2011).

[3] D. Narducci, E. Selezneva, G. Cerofolini, S. Frabboni, and G. Ottaviani, "Impact of energy filtering and carrier localization on the thermoelectric properties of granular semiconductors," J. Solid State Chem. **193**, 19 (2012).

[4] Y. Lan, A. J. Minnich, G. Chen, and Z. Ren, "Enhancement of thermoelectric figure-of-merit by a bulk nanostructuring approach," Adv. Funct. Mater. **20**, 357 (2010).

[5] L. D. Zhao, S.-H. Lo, Y. Zhang, H. Sun, G. Tan, C. Uher, C. Wolverton, V. P. Dravid, and M. G. Kanatzidis, "Ultralow thermal conductivity and high thermoelectric figure of merit in SnSe crystals," Nature (London) **508**, 373 (2014).

[6] H. J. Wu, L.-D. Zhao, F. S. Zheng, D. Wu, Y. L. Pei, X. Tong, M. G. Kanatzidis, and J. Q. He, "Broad temperature plateau for thermoelectric figure of merit ZT>2 in phase-separated $PbTe_{0.7}S_{0.3}$," Nat. Commun. **5**, 4515 (2014).

[7] D. Ginting, C.-C. Lin, R. Lydia, H. S. So, H. Lee, J. Hwang, W. Kim, R. A. R. A. Orabi, and J.-S. Rhyee, "High thermoelectric performance in pseudo quaternary compounds of $(PbTe)_{0.95-x}(PbSe)_x(PbS)_{0.05}$ by simultaneous band convergence and nano precipitation," Acta Mater. **131**, 98 (2017).

[8] C.-C. Lin, R. Lydia, J. H. Yun, H. S. Lee, and J.-S. Rhyee, "Extremely low lattice thermal conductivity and point defect scattering of phonons in Ag-doped $(SnSe)_{1-x}(SnS)_x$ compounds," Chem. Mater. **29**, 5344 (2017).

[9] D. T. Morelli, V. Jovovic, and J. P. Heremans, "Intrinsically minimal thermal conductivity in cubic I-V-VI$_2$ semiconductors," Phys. Rev. Lett. **101**, 035901 (2008).

[10] M. D. Nielsen, V. Ozolins, and J. P. Heremans, "Lone pair electrons minimize lattice thermal conductivity," Energy Environ. Sci. **6**, 570 (2013).

[11] H.-J. Wu, P.-C. Wei, H.-Y. Cheng, J.-R. Deng, and Y.-Y. Chen, "Ultralow thermal conductivity in n-type Ge-doped AgBiSe$_2$ thermoelectric materials," Acta Mater. **141**, 217 (2017).

[12] S. Roychowdhury, R. Panigrahi, S. Perumal, and K. Biswas, "Ultrahigh thermoelectric figure-of-merit and enhanced mechanical stability of p-type $AgSb_{1-x}Zn_xTe_2$," ACS Energy Lett. **2**, 349 (2017).

[13] S. N. Guin and K. Biswas, "Sb deficiencies control hole transport and boost the thermoelectric performance of p-type AgSbSe$_2$," J. Mater. Chem. C **3**, 10415 (2015).

[14] Z. Liu, J. Shuai, H. Geng, J. Mao, Y. Feng, X. Zhao, X. Meng, R. He, W. Cai, and J. Sui, "Contrasting the role of Mg and Ba doping on the microstructure and thermoelectric properties of p-Type AgSbSe$_2$," ACS Appl. Mater. Interf. **7**, 23047 (2015).

[15] S. N. Guin, A. Chatterjee, and K. Biswas, "Enhanced thermoelectric performance in p-type AgSbSe$_2$ by Cd-doping," RSC Adv. **4**, 11811 (2014).

[16] M. K. Jana, K. Pal, U. V. Waghmare, and K. Biswas, "The origin of ultralow thermal conductivity in InTe: lone-pair-induced anharmonic rattling," Angew Chem. Int. Ed. **55**, 7792 (2017).

[17] T. Chattopadhyay, R. P. Santandrea, and H. G. Von Schnering, "Temperature and pressure dependence of the crystal structure of InTe: A new high pressure phase of InTe," J. Phys. Chem. Solids **46**, 351 (1985).

[18] G. Kresse and J. Hafner, "Ab initio molecular-dynamics simulation of the liquid-metal–amorphous-semiconductor transition in germanium," Phys. Rev. B **49**, 14251 (1994).

[19] G. Kresse and J. Furthmüller, "Efficient iterative schemes for ab initio total-energy calculations using a plane-wave basis set," Phys. Rev. B **54**, 11169 (1996).

[20] G. Kresse and J. Furthmüller, "Efficiency of ab-initio total energy calculations for metals and semiconductors using a plane-wave basis set," Comput. Mater. Sci. **6**, 15 (1996).

[21] P. E. Blöchl, "Projector augmented-wave method," Phys. Rev. B **50**, 17953 (1994).

[22] J. P. Perdew, K. Burke, and M. Ernzerhof, "Generalized gradient approximation made simple," Phys. Rev. Lett. **77**, 3865 (1996).

[23] M. Methfessel and A. T. Paxton, "High-precision sampling for Brillouin-zone integration in metals," Phys. Rev. B **40**, 3616 (1989).

[24] P. E. Blöchl, O. Jepsen, and O. K. Andersen, "Improved tetrahedron method for Brillouin-zone integrations," Phys. Rev. B **49**, 16223 (1994).

[25] W. Setyawan and S. Curtarolo, "High-throughput electronic band structure calculations: Challenges and tools," Comput. Mater. Sci. **49**, 299 (2010).

[26] C. Kittel, *Introduction to Solid State Physics* (8th Ed.), John Wiley & Sons, Inc., p. 112 (2005).

[27] J. Shuai, J. Mao, S. Song, Q. Zhu, J. Sun, Y. Wang, R. He, J. Zhou, G. Chen, D. J. Singh, and Z. Ren, "Tuning the carrier scattering mechanism to effectively improve the thermoelectric properties," Energy Environ. Sci. **10**, 799 (2017).

[28] G. J. Snyder and E. S. Toberer, Nat. Mater. **7**, 105 (2008).

[29] F. M. Andrew and G. J. Snyder, Introduction to modeling thermoelectric transport at high temperatures, materials, preparation, and characterization in thermoelectrics (CRC Press, New York, 2012), pp. 1–18.

[30] C.-C. Lin, D. Ginting, R. Lydia, M. H. Lee, and J.-S. Rhyee, "Thermoelectric properties and extremely low lattice thermal conductivity in p-type Bismuth Tellurides by Pb-doping and PbTe precipitation," J. Alloys Compd. **671**, 538 (2016).

[31] D. T. Morelli and J. P. Heremans, "Thermal conductivity of germanium, silicon, and carbon nitrides," Appl. Phys. Lett. **81**, 5126 (2002).